

# Anti-CEA Pretargeted Immuno-PET Shows Higher Sensitivity Than DOPA PET/CT in Detecting Relapsing Metastatic Medullary Thyroid Carcinoma: Post Hoc Analysis of the iPET-MTC Study

Caroline Bodet-Milin<sup>1</sup>, Alain Faivre-Chauvet<sup>1</sup>, Thomas Carlier<sup>1</sup>, Catherine Ansquer<sup>1</sup>, Aurore Rauscher<sup>2</sup>, Eric Frampas<sup>1-3</sup>, Frederique Toulgoat<sup>3</sup>, Damien Masson<sup>4</sup>, Mickael Bourgeois<sup>1</sup>, Evelyne Cerato<sup>5</sup>, Vincent Rohmer<sup>6</sup>, Olivier Couturier<sup>7</sup>, Delphine Drui<sup>8</sup>, David M. Goldenberg<sup>9</sup>, Robert M. Sharkey<sup>10</sup>, Jacques Barbet<sup>11</sup>, and Françoise Kraeber-Bodere<sup>1</sup>

<sup>1</sup>Université de Nantes, CHU Nantes, CNRS, INSERM, CRCINA, Nantes, France; <sup>2</sup>Pharmacy Unit, ICO Cancer Center, Saint-Herblain, France; <sup>3</sup>Radiology Department, University Hospital, Nantes, France; <sup>4</sup>Biology Department, University Hospital, Nantes, France; <sup>5</sup>Délégation à la Recherche Clinique et à l'Innovation, University Hospital, Nantes, France; <sup>6</sup>Endocrinology Department, University Hospital, Angers, France; <sup>7</sup>Nuclear Medicine Department, University Hospital, Angers, France; <sup>8</sup>Endocrinology Department, University Hospital, Nantes, France; <sup>9</sup>IBC Pharmaceuticals, Inc., Morris Plains, New Jersey; <sup>10</sup>Immunomedics, Inc., Morris Plains, New Jersey; and <sup>11</sup>GIP Arronax, Saint-Herblain, France

J Nucl Med 2021; 62:1221–1227

DOI: 10.2967/jnumed.120.252791

Pretargeting parameters for the use of anti-carcinoembryonic antigen (CEA) bispecific monoclonal antibody TF2 and the <sup>68</sup>Ga-labeled IMP288 peptide for immuno-PET have been optimized in a first-in-humans study performed on medullary thyroid carcinoma (MTC) patients (the iPET-MTC study). The aim of this post hoc analysis was to determine the sensitivity of immuno-PET in relapsing MTC patients, in comparison with conventional imaging and <sup>18</sup>F-L-dihydroxyphenylalanine (<sup>18</sup>F-DOPA) PET/CT. **Methods:** Twenty-five studies were analyzed in 22 patients. All patients underwent immuno-PET 1 and 2 h after <sup>68</sup>Ga-IMP288 injection pretargeted by TF2, in addition to neck, thoracic, abdominal, and pelvic CT; bone and liver MRI; and <sup>18</sup>F-DOPA PET/CT. The gold standard was histology or confirmation by one other imaging method or by imaging follow-up. **Results:** In total, 190 lesions were confirmed by the gold standard: 89 in lymph nodes, 14 in lungs, 46 in liver, 37 in bone, and 4 in other sites (subcutaneous tissue, heart, brain, and pancreas). The number of abnormal foci detected by immuno-PET was 210. Among these, 174 (83%) were confirmed as true-positive by the gold standard. Immuno-PET showed a higher overall sensitivity (92%) than <sup>18</sup>F-DOPA PET/CT (65%). Regarding metastatic sites, immuno-PET had a higher sensitivity than CT, <sup>18</sup>F-DOPA PET/CT, or MRI for lymph nodes (98% vs. 83% for CT and 70% for <sup>18</sup>F-DOPA PET/CT), liver (98% vs. 87% for CT, 65% for <sup>18</sup>F-DOPA PET/CT, and 89% for MRI), and bone (92% vs. 64% for <sup>18</sup>F-DOPA PET/CT and 86% for MRI), whereas sensitivity was lower for lung metastases (29% vs. 100% for CT and 14% for <sup>18</sup>F-DOPA PET/CT). Tumor SUV<sub>max</sub> at 60 min ranged from 1.2 to 59.0, with intra- and interpatient variability. **Conclusion:** This post hoc study demonstrates that anti-carcinoembryonic antigen immuno-PET is an effective procedure for detecting metastatic MTC lesions. Immuno-PET showed a higher overall sensitivity than <sup>18</sup>F-DOPA PET/CT for disclosing metastases, except for the lung, where CT remains the most effective examination.

**Key Words:** immuno-PET; MTC; carcinoembryonic antigen; bispecific antibody; pretargeted radioimmunoimaging

**M**edullary thyroid carcinoma (MTC) arises from calcitonin-producing parafollicular C cells and represents 1%–2% of thyroid cancers (1). The tumor is frequently aggressive; on initial staging, 35% of MTC patients have tumor extending into the thyroid-surrounding tissues or regional lymph node involvement, and 13% have distant metastases, especially in the lung, liver, or bones (2,3). According to American Thyroid Association guidelines, when calcitonin is higher than 150 pg/mL, anatomic imaging-based staging is recommended, such as neck ultrasonography or CT, chest CT, liver CT or MRI, and spine and pelvis bone or bone marrow MRI (4,5). As indolent tumors, MTCs have a generally low avidity for <sup>18</sup>F-FDG; therefore, PET with <sup>18</sup>F-FDG is not recommended for initial staging but can be useful for assessing advanced disease characterized by dedifferentiation and rapid progression. <sup>18</sup>F-L-dihydroxyphenylalanine (<sup>18</sup>F-DOPA) PET/CT has a higher sensitivity and specificity than <sup>18</sup>F-FDG PET/CT in MTC and can reveal occult metastases or small lesions for initial staging and at relapse. These examinations also can play a crucial role in the management of relapsing MTC patients (6–12).

Carcinoembryonic antigen (CEA) is a cell-surface glycoprotein overexpressed in several solid tumors, including MTC, and functional imaging using radiolabeled anti-CEA monoclonal antibodies represents a potentially interesting method for detection of MTC metastases (13). TF2 is an engineered bispecific monoclonal antibody (BsMAb) comprising an antihapten Fab fragment derived from the murine 679 antibody recognizing the histamine-succinyl-glycine motif, as well as 2 humanized anti-CEA Fab fragments derived from the hMN-14 antibody (labetuzumab), formed into a trivalent 157-kD protein by the Dock-and-Lock (Immunomedics) procedure (14). IMP288 is a bivalent histamine-succinyl-glycine hapten that can be labeled with a variety of radionuclides for

Received Jul. 8, 2020; revision accepted Jan. 13, 2021.  
For correspondence or reprints, contact Caroline Bodet-Milin (caroline.milin@chu-nantes.fr).  
Published online February 5, 2021.  
COPYRIGHT © 2021 by the Society of Nuclear Medicine and Molecular Imaging.

therapy ( $^{90}\text{Y}$  and  $^{177}\text{Lu}$ ), scintigraphy ( $^{111}\text{In}$ ), or PET ( $^{124}\text{I}$ ,  $^{68}\text{Ga}$ , and  $^{18}\text{F}$ ) (15–17).

We previously reported the optimization of the pretargeting parameters (BsmAb and peptide molar doses and pretargeting delay) of pretargeted immuno-PET using TF2 and  $^{68}\text{Ga}$ -IMP288 in the iPET-MTC first-in-humans study performed on MTC patients (18). The aim of this post hoc analysis was to determine the sensitivity of this novel imaging method in relapsing MTC patients, in comparison to conventional imaging and  $^{18}\text{F}$ -DOPA PET/CT.

## MATERIALS AND METHODS

### Population

The inclusion and exclusion criteria have been reported previously (18). Briefly, all eligible adult patients had a histologic diagnosis of MTC treated by complete surgery and presenting a calcitonin serum level of 150 pg/mL or more with at least 1 lesion 10 mm or greater on conventional imaging. In the 4 wk preceding immuno-PET, a staging workup that included a complete history, physical examination, CEA and calcitonin serum level measurements, and  $^{18}\text{F}$ -DOPA PET/CT was performed for each patient. Conventional imaging, including contrast-enhanced CT of the neck, chest, abdomen, and pelvis, as well as bone and liver MRI, was performed. The iPET-MTC trial, sponsored by Nantes University Hospital, was approved by the responsible ethics committee (comité de protection des personnes) and registered at ClinicalTrials.gov (NCT01730638), and all patients gave written informed consent.

### Investigational Agents and Study Design

Radiopharmaceutical manufacturing and premedication protocols have been previously reported (18). For pharmacokinetics optimization, the first 16 immuno-PET studies were performed under 5 different pretargeting conditions (molar doses of BsmAb and peptide, and delay); 3 patients were included per cohort from cohorts 1 to 5 (18). One patient included in the third cohort did not receive the full hapten dose and was excluded and replaced in the optimization phase of the study. This patient was reintegrated in this part of the study evaluating the performance of immuno-PET. The last 9 immuno-PET studies were performed with the cohort 2 scheme considered as optimal after the optimization phase (Table 1).

Safety was assessed by monitoring vital signs, physical examination findings, and adverse events. Human antihuman antibody titers were measured by Immunomedics at 3 or 6 mo, using an enzyme-linked immunosorbent assay (abnormal when  $\geq 50$  ng/mL).

### PET Acquisition

Immuno-PET and  $^{18}\text{F}$ -DOPA PET/CT were performed using a 4-ring Siemens Biograph mCT system and reconstructed using 3-dimensional ordinary Poisson ordered-subsets expectation maximization with point-spread-function correction and time-of-flight mode (3 iterations, 21 subsets, gaussian postfiltering of 2 mm in full width at half maximum, voxel size of  $4 \times 4 \times 2$  mm). Whole-body acquisitions were performed under normal tidal respiration for 2.5 min per bed position. CT was performed using a variable mAs, 120 kVp, and a pitch of 1 without contrast enhancement. Acquisitions were performed from the top of the head to the mid thigh (6–8 steps per patient). Immuno-PET was performed 60 and 120 min after a 150-MBq injection of  $^{68}\text{Ga}$ -IMP288, and  $^{18}\text{F}$ -DOPA PET/CT was performed 60 min after a 3 MBq/kg injection of  $^{18}\text{F}$ -DOPA.

### Conventional Imaging Acquisition

Patients were scanned with multidetector CT. A contrast-enhanced series was acquired after intravenous injection of nonionic iodinated contrast medium (350 mL, 1.5 mL/kg, rate of 3 mL/s using a power injector), visualizing the body from the neck to the pelvis. MRI was conducted using a 1.5-T whole-body MRI system. The liver was imaged in the axial plane using T2-weighted, MR diffusion-weighted sequences and transverse breath-hold 3-dimensional T1-weighted fat-suppressed spoiled gradient-recalled-echo sequences before and after administration of gadolinium chelate. The standard MR sequences for spine and pelvis included T1-weighted turbo spin-echo, T2-weighted short-T1 inversion recovery with fat suppression, and contrast-enhanced T1-weighted turbo spin-echo with fat suppression. The whole spine was explored in sagittal views with or without complementary axial views and the pelvis in coronal and axial views.

### Image Analysis

Abnormal uptake on immuno-PET was defined as a focal increase visually higher than the surrounding background level. Attenuation-correction CT data were used in addition to PET data for interpretation of the immuno-PET and  $^{18}\text{F}$ -DOPA PET/CT findings. Tumor  $\text{SUV}_{\text{max}}$  was determined on the most intense focus confirmed as MTC in the whole-body scan.  $^{18}\text{F}$ -DOPA PET/CT and immuno-PET were interpreted separately by 2 nuclear medicine physicians who did not know the other diagnostic results and had expertise in immunotargeting and PET.

Conventional imaging findings were interpreted by a consensus of radiologists with expertise in endocrine tumors, who were unaware of the  $^{18}\text{F}$ -DOPA PET/CT and immuno-PET results but could consider the results of previous conventional imaging. At initial conventional imaging, lesions were considered metastatic in any of the following 5

**TABLE 1**  
Scheme of Cohorts

Cohort	Patients (n)	TF2 dose (nmol)	Delay (h)	$^{68}\text{Ga}$ -IMP288 dose and activity (nmol)	MBq	TF2/IMP288 molar dose ratio
I	3	120	24	6	150	20
II	3 + 9*	120	30	6	150	20
III	3 + 1†	120	42	6	150	20
IV	3	120	30	3	150	40
V	3	60	30	3	150	20

\*Three patients in optimization phase of study and 9 in validation phase.

†Patient 8 did not receive full hapten dose and was excluded and replaced for optimization phase study but was reintegrated for sensitivity study.

cases: first, if there were pulmonary nodules on chest CT; second, if there were focal hepatic lesions (hyperintense at a high b value on diffusion-weighted MRI, moderately to strongly hyperintense on T2-weighted MRI [less than the signal intensity of liquid], or hypervascular or peripherally enhanced after contrast injection on MRI or CT); third, if there was hyperintensity on T2- and diffusion-weighted MRI, hypointensity on T2- and T1-weighted MRI, or mixed heterogeneous intensity on MRI; fourth, if there was a short-axis (>1 cm) or hypervascular pattern of lymph nodes; and fifth, if there were soft-tissue tumors. The appearance of new lesions during the course of the disease and an increase in size during follow-up were also considered.

For both ethical and practical reasons, not every suspected lesion was evaluated by histology. If necessary, complementary imaging was performed to assess the most important lesions suspected by immuno-PET and not detected by the initial work-up. For this study, the gold standard was determined on the basis of histology, by confirmation of a lesion by one other imaging method, or by imaging follow-up. Indeed, an imaging assessment with contrast-enhanced CT of the neck, chest, abdomen, and pelvis or bone MRI, liver MRI, or <sup>18</sup>F-DOPA PET/CT was performed 3 mo after immuno-PET, decided by a panel of experts involving endocrinologists, radiologists, and nuclear physicians. CEA and calcitonin serum levels were also measured. The same panel of experts could propose a second biomarker and imaging evaluation at 6 mo after immuno-PET. RECIST or the criteria of the European Organization for Research and Treatment of Cancer were used for conventional imaging follow-up (19,20).

A lesion detected by an imaging method was considered related to MTC (true-positive) when confirmed by one other imaging method, by histopathology, or by follow-up. A lesion visualized by one imaging method and progressing during follow-up using RECIST or the criteria of the European Organization for Research and Treatment of Cancer was considered true-positive. A negative finding on an imaging method was considered false-negative if positive by one other imaging method plus histopathology or by one other imaging method plus follow-up. Sensitivity [(true-positive/true-positive + false-negative) × 100] per lesion was calculated for each imaging modality. A positive finding on an imaging method was considered unconfirmed if not confirmed either by one other imaging method or by follow-up or histopathology. A positive finding on an imaging method was considered false-positive if not confirmed as positive by histopathology.

The Wilcoxon rank sum test was used to compare median tumor SUV<sub>max</sub> and median tumor SUV<sub>max</sub>-to-mediastinal blood pool ratio at 60 or 120 min, and the Spearman test was used to evaluate whether SUV<sub>max</sub> was associated with CEA or calcitonin levels.

## RESULTS

### Patient Characteristics and Adverse Events

The characteristics of the 22 included patients are presented in Table 2. Three patients underwent a second immuno-PET study at least 12 mo after the first procedure, coupled with conventional imaging or DOPA PET/CT, accounting for a total of 25 immuno-PET, conventional imaging, or DOPA PET/CT studies in the 22 patients. Pathologic lesions were histopathologically analyzed in 6 patients (2 noncontributory biopsies, 3 biopsies confirming MTC metastases, and 1 biopsy diagnosing another disease).

No patient experienced an anaphylactic reaction during or after the TF2 infusion. One patient experienced a grade 3 reaction starting immediately after the hapten infusion, with malaise, bronchospasm, tachycardia, and hypertension, requiring hospitalization. Therefore, the protocol was amended, and a premedication with antihistamine and corticosteroid before both TF2 and IMP288

**TABLE 2**  
Patient Characteristics

Characteristic	Data
Total patients	22
Age (y)	62 (28–75)
Sex	
Male	15
Female	7
Time from diagnosis (y)	5.5 (0.5–31)
Calcitonin concentration (pg/mL)	488 (154–39,000)
CEA concentration (ng/mL)	18 (3–1,443)
Location of disease	
Lymph node	19
Lung	8
Liver	13
Bone	13
Other	4

Qualitative data are number; continuous data are median and range.

injections was given thereafter to all patients. No further allergic reactions occurred afterward.

Human antihuman antibody was analyzed in 19 patients (at 3 and 6 mo in 14 patients and only at 3 mo in 5 patients). Three patients had abnormal human antihuman antibody. In 2 of those patients, the level was abnormal at 3 mo (52 and 152 ng/mL) but had normalized by 6 mo. In the third patient, the level was normal at 3 mo but abnormal at 6 mo (244 ng/mL).

### Imaging Results and Sensitivity

All patients had abnormalities detected by immuno-PET, conventional imaging, or <sup>18</sup>F-DOPA PET/CT (Table 3). In total, 190 lesions were confirmed according to the definition of the gold standard: 89 in lymph nodes, 14 in the lungs, 46 in the liver, 37 in bone or bone marrow, and 4 at other sites (subcutaneous tissue, heart, brain, and pancreas). Among these 190 lesions validated by the gold standard, 174 were confirmed by another imaging method, 13 by follow-up, and 3 by histology. Immuno-PET detected a total of 210 abnormal foci (1–22 per patient). Among these, 174 (83%) were confirmed as true-positive according to the gold standard (167 by another imaging method, 4 by follow-up, and 3 by histology). Sixteen lesions were missed (false-negative lesions): 10 in the lungs, 3 in bone, 2 in lymph nodes, and 1 in the liver (Table 3). All immuno-PET lesions were seen at both 60 and 120 min. Tumor SUV<sub>max</sub> at 60 min ranged from 1.2 to 59.0, with intra- and interpatient variability (Fig. 1). There was no significant difference between median tumor SUV<sub>max</sub> and median tumor SUV<sub>max</sub>-to-mediastinal blood pool ratio at 60 or 120 min (19.54 [range, 4.09–94.14] vs. 21.31 [range, 5.14–100.2] [*P* = 0.84] and 8.14 [range, 1.39–34.1] vs. 8.5 [range, 2.7–49.6] [*P* = 0.75], respectively). SUV<sub>max</sub> was not associated with CEA or calcitonin serum levels (Spearman *P* = 0.71 and 0.73, respectively).

CT, <sup>18</sup>F-DOPA PET/CT, liver MRI, and bone marrow MRI detected 130, 124, 41, and 33 true-positive lesions, respectively, and

**TABLE 3**  
Sensitivity of Immuno-PET, <sup>18</sup>F-DOPA PET/CT, and Conventional Imaging

Location	Immuno-PET	<sup>18</sup> F-DOPA PET/CT	CT	Liver MRI	Bone marrow MRI
Nodes	87/89 (98%)	64/89 (72%)	73/89 (82)%	NA	NA
Lung	4/14 (29%)	2/14 (14%)	14/14 (100%)	NA	NA
Liver	45/46 (98%)	30/46 (65%)	39/46 (87%)	41/46 (89%)	NA
Bone marrow	34/37 (92%)	25/37 (68%)	NA	NA	33/37 (89%)
Other	4/4 (100%)	3/4 (75%)	4/4 (100%)	NA	NA
Global	174/190 (92%)	124/190 (65%)	130/153 (85%)	NA	NA

NA = not applicable.

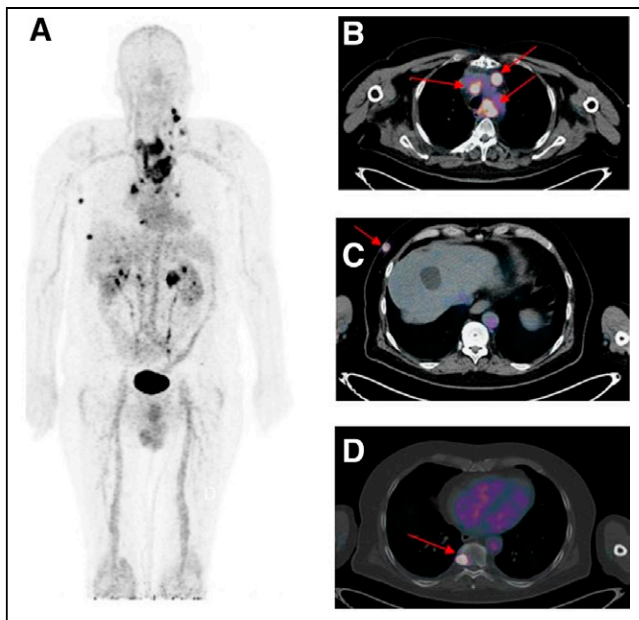


**FIGURE 1.** Immuno-PET/CT with anti-CEA BsmAb and <sup>68</sup>Ga-IMP288 peptide showing pathological lesions with heterogeneous SUV<sub>max</sub> ranging from 3.0 to 20.1. Maximum-intensity-projection (MIP) image (A) showed several pathological lesions. On the fusion axial images, arrows located mediastinal nodes (B), subcutaneous lesions (C), and bone metastasis (D).

missed 23, 66, 5, and 4 lesions (Table 3). Subcutaneous, pancreatic, and heart lesions were detected by immuno-PET, conventional imaging, and <sup>18</sup>F-DOPA PET/CT, whereas a brain lesion was depicted by immuno-PET and confirmed by brain MRI but not detected by <sup>18</sup>F-DOPA PET/CT (Fig. 2). No lesion was considered false-positive by immuno-PET, but 36 lesions remained not confirmed. For <sup>18</sup>F-DOPA PET/CT, 7 lesions remained not confirmed and 1 was false-positive: a diffuse area of pathologic bone marrow uptake was described on <sup>18</sup>F-DOPA PET/CT, whereas Vaquez polycythemia was diagnosed without MTC metastases on bone marrow biopsy. Bone MRI was also false-positive in this patient, whereas immuno-PET was negative. For CT, 7 lesions were not confirmed (1 peritoneal nodule and 6 lung micronodules). Supplemental Table 1 summarizes the per-patient performance of immuno-PET, <sup>18</sup>F-DOPA PET/CT, CT, liver MRI, and bone MRI (supplemental materials are available at <http://jnm.snmjournals.org>).

Immuno-PET showed a higher overall sensitivity (92%) than <sup>18</sup>F-DOPA PET/CT (65%) (Table 3). The sensitivity of immuno-PET was also 92% (79/86) considering only the 13 exams performed with the suboptimal scheme. Regarding the different metastatic sites, immuno-PET had a higher sensitivity than CT or <sup>18</sup>F-DOPA PET/CT for lymph nodes (98% vs. 82% and 72%, respectively) (Fig. 3) and liver (98% vs. 87% and 65%, respectively) (Fig. 4), whereas sensitivity was lower for lung metastases (29% vs. 100% and 14%, respectively). Immuno-PET had a slightly higher sensitivity for bone evaluation than MRI or <sup>18</sup>F-DOPA PET/CT (92% vs. 89% and 68%, respectively).

#### DISCUSSION

Currently, surgery remains the only treatment for cure of MTC patients. Once the disease is metastatic, the therapeutic options are limited. MTC cells do not concentrate radioiodine, and the efficacy of chemotherapeutic agents is limited (4). In the last decade, tyrosine kinase inhibitors have been evaluated in patients with progressive metastatic disease, with benefits on progression-free survival for both vandetanib and cabozantinib (21). Locally advanced or relapsing MTC requires a careful work-up, including a work-up of calcitonin and CEA serum level measurements and determination of their doubling time, as well as comprehensive imaging to determine the extent of the disease, its aggressiveness, and whether therapy is needed. Calcitonin is the most sensitive and specific tumor biomarker, and CEA represents a prognostic biomarker because an increased CEA serum level suggests an advanced state and tumor dedifferentiation (22). Serum calcitonin and CEA doubling times are prognostic of survival (21,23). Morphologic imaging is often negative or doubtful in the presence of rising levels of calcitonin (3–5). Therefore, functional PET/CT imaging using different radiopharmaceuticals is recommended. <sup>18</sup>F-DOPA seems to be the most useful tracer to detect recurrent MTC based on rising biomarker levels, whereas <sup>18</sup>F-FDG may be complementary in patients with an aggressive tumor phenotype (3,5,8,11,24).

The present study found a high imaging performance for anti-CEA TF2 BsmAb and <sup>68</sup>Ga-IMP288 in patients who have metastatic MTC, with immuno-PET achieving a 92% overall sensitivity—somewhat better than the sensitivity of conventional imaging and <sup>18</sup>F-DOPA PET/CT for lymph node, liver, and bone or bone marrow examinations. However, as in a previous study on breast cancer patients, immuno-PET was less effective than CT for lung metastasis detection (25). The sensitivity of <sup>18</sup>F-DOPA PET/CT also was low for lung lesion detection in this population. Spontaneous breathing during the PET/CT acquisition and the large positron range of <sup>68</sup>Ga may affect

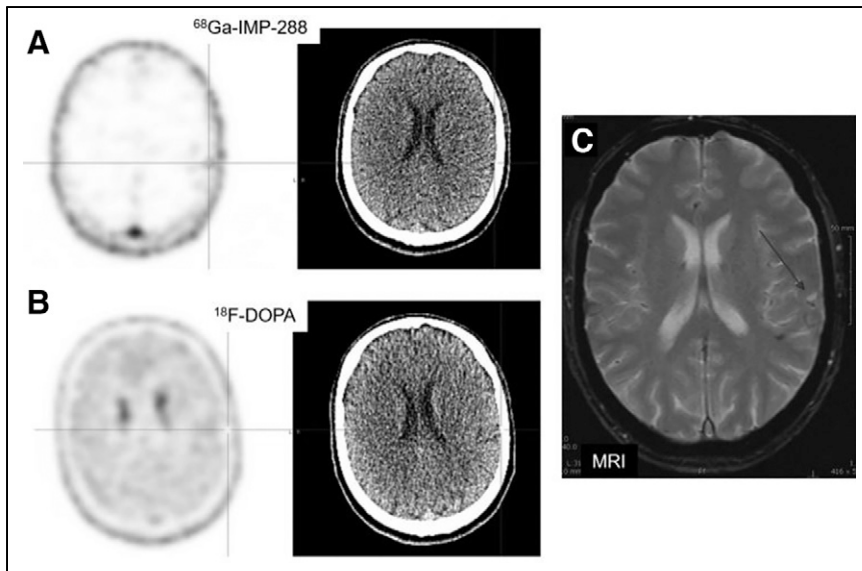


**FIGURE 2.** (A) Immuno-PET images with anti-CEA BsmAb and  $^{68}\text{Ga}$ -IMP288 showing temporoparietal uptake in brain. CT of the PET/CT was negative. (B) PET/CT with  $^{18}\text{F}$ -DOPA PET/CT was negative. (C) Brain MRI (guided by immuno-PET) confirmed pathologic temporoparietal lesion (arrow).

the ability of PET to detect small lung lesions. Indeed, the sensitivity of immuno-PET was better than that of  $^{18}\text{F}$ -DOPA PET/CT both overall and for metastatic sites, suggesting that this novel functional whole-body imaging method may be of interest for MTC staging and therapeutic evaluation. Excluding lung lesions only 6 lesions (3 in bone, 2 in lymph nodes, and 1 in liver) in 4 patients were false-negative on immuno-PET when all other MTC metastases were positive on immuno-PET. Two of these 6 lesions (1 bone lesion and 1 node lesion) were

significantly upregulated in neuroendocrine tumors, including MTC. In a metaanalysis including 8 studies and 146 patients, the detection rates of  $^{18}\text{F}$ -DOPA PET and PET/CT, by per-patient and per-lesion analyses, were 66% and 71%, respectively, with performance increasing in patients with a serum calcitonin level of at least 1,000 ng/L and a calcitonin doubling time of less than 24 mo (26).

$^{18}\text{F}$ -FDG is a glucose metabolism tracer, with increased uptake in MTCs undergoing dedifferentiation and becoming more aggressive

positive using  $^{18}\text{F}$ -DOPA. The small size of these lesions, in addition to the spontaneous breathing during the PET/CT acquisition, may affect PET performance because of the partial-volume effect. A heterogeneous expression of CEA on some metastatic lesions might also explain these false-negative immuno-PET results. The  $^{18}\text{F}$ -DOPA PET/CT results—with a higher number of false-negative lesions (16 for immuno-PET vs. 66 for  $^{18}\text{F}$ -DOPA PET/CT)—had no impact on patient staging in this study, suggesting that immuno-PET could potentially replace  $^{18}\text{F}$ -DOPA PET/CT in patients with metastatic MTC if the technique were available in clinical practice.

In clinical practice,  $^{18}\text{F}$ -DOPA,  $^{18}\text{F}$ -FDG, and somatostatin analogs labeled with  $^{68}\text{Ga}$  are available to explore MTC patients with an increasing calcitonin serum level.  $^{18}\text{F}$ -DOPA penetrates into tumor cells through transmembrane amino acid transporters that are significantly

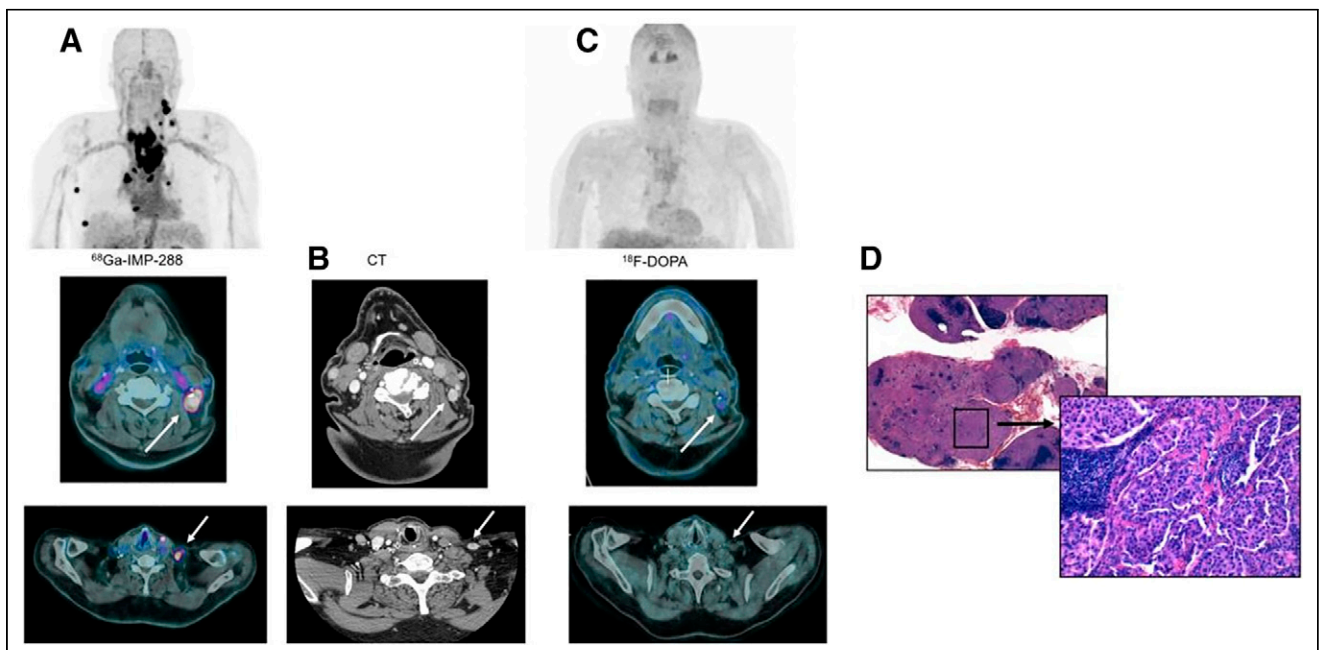


**FIGURE 3.** (A) Immuno-PET/CT with anti-CEA BsmAb and  $^{68}\text{Ga}$ -IMP288 maximum-intensity-projection (MIP) showing multiple pathologic lesions confirmed to be cervical and mediastinal nodes on the fusion axial images (arrows). (B) Pathological nodes were confirmed on contrast-enhanced CT (arrows) but not visualized by MIP or fusion axial  $^{18}\text{F}$ -DOPA PET/CT images (C). (D) Metastatic MTC involvement was confirmed by histologic analysis (hematoxylin/eosin/saffron staining,  $\times 12.5$  and  $\times 200$ ).

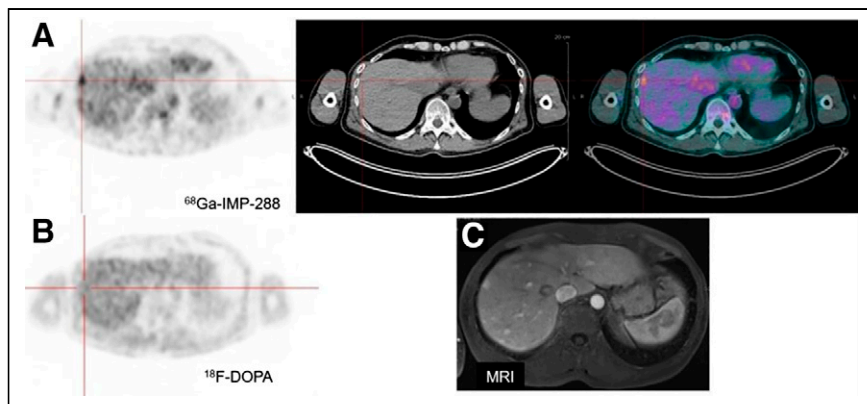


**FIGURE 4.** (A) Immuno-PET/CT with anti-CEA BsmAb and  $^{68}\text{Ga}$ -IMP288 axial PET, CT, and fusion images showing multiple liver lesions (arrows), whereas  $^{18}\text{F}$ -DOPA PET was negative (B). (C) MRI-confirmed lesion.

(5). A metaanalysis based on 24 studies comprising 538 patients with suspected recurrent MTC found, using a per-patient-based analysis, that  $^{18}\text{F}$ -FDG PET or PET/CT had a detection rate of 59%, with performance increasing when serum calcitonin was at least 1,000 ng/L, CEA at least 5 ng/mL, calcitonin doubling time less than 12 mo, and CEA doubling time less than 24 mo (26). Neuroendocrine tumors usually overexpress somatostatin receptors, and somatostatin analogs labeled with  $^{68}\text{Ga}$  are useful for their assessment. A recent prospective study evaluating  $^{68}\text{Ga}$ -DOTATATE PET/CT in 30 MTC patients showed that it was inferior to conventional imaging, except for bone scans (27), in patients with metastatic disease. The sensitivity of  $^{68}\text{Ga}$ -DOTATATE PET/CT was 56%, 57%, and 9% for detecting neck lymph nodes, lung metastases, and liver metastases, respectively, and 100% for bone metastases.

Even if no comparative studies have been done on homogeneous populations, our results suggest that, except for lung metastasis detection, anti-CEA pretargeted immuno-PET may have a higher performance than other available PET/CT methods and conventional imaging to detect recurrence in MTC patients with rising serum biomarkers. Our previous studies showed that CEA expression seemed to be almost constant in MTC and that high-sensitivity PET imaging using CEA as a target would detect the disease independently of the prognosis (9,28–30).

Despite the excellent sensitivity of pretargeted immuno-PET, our study had some limitations. Only a small number of patients were included. This limited number is explained on the one hand by the relative rarity of the tumor concerned and on the other hand by our intention to test this new pretargeting system in parallel in MTC and breast cancer patients (24). Moreover, we evaluated the performance of immuno-PET in the whole population and not only for the 12 examinations performed under the optimal pretargeting conditions defined by the optimization study. This bias could penalize us because 13 procedures were performed under suboptimal conditions; however, the sensitivity of immuno-PET was the same in this subgroup as in the overall population (92%). The absence of a systematic early acquisition time for  $^{18}\text{F}$ -DOPA PET/CT—although  $^{18}\text{F}$ -DOPA clearance can sometimes be fast in this tumor—could also represent a bias and explain why the global sensitivity of  $^{18}\text{F}$ -DOPA PET/CT was slightly lower than usually reported in the literature (12).

Finally, and this bias is recurrent in many imaging studies, 36 lesions detected by immuno-PET remained unconfirmed by the gold standard during the follow-up period. Although the gold

standard had a relatively extensive definition, not all lesions could be confirmed. Indeed, immuno-PET visualized more lesions than the other modalities—lesions that were often very small, not confirmed by conventional assessment, and inaccessible to histologic analysis. Only 6 biopsies were performed in our study, 2 being non-contributory, 3 confirming the MTC metastases, and 1 diagnosing another disease. This lack of confirmation does not allow an accurate assessment of the positive predictive value and specificity of this new imaging technique.

Pretargeted immuno-PET could also be a theranostic procedure for qualitative and quantitative whole-body tumor biomarker cartography to

select candidates for antibody-based therapy. Our team reported promising results for radionuclide therapy using a previous generation of pretargeting reagents (anti-CEA  $\times$  anti-diethylentriaminepentacetic acid [DTPA] BsmAb hMN-14  $\times$  m734 and  $^{131}\text{I}$ -di-DTPA-indium hapten) (28–31). In 42 patients with metastatic, progressing MTC included in a phase II study, a 76.2% disease control rate (durable stabilization plus objective response) was observed (2). Using the new-generation IMP288 peptide, the feasibility and safety of theranostics using TF2 and  $^{111}\text{In}/^{177}\text{Lu}$ -IMP288 have been reported in metastatic colorectal and lung cancer patients (32,33). Moreover, anti-CEA antibody–drug conjugates are under preclinical and clinical development, and immuno-PET using  $^{68}\text{Ga}$ -IMP288 might be able to select patients for these therapeutic strategies (34,35).

## CONCLUSION

This post hoc analysis demonstrated that anti-CEA immuno-PET using the trivalent BsmAb TF2 and the  $^{68}\text{Ga}$ -IMP288 peptide is a safe and effective procedure for detecting metastatic MTC lesions. Immuno-PET targeting CEA showed a higher overall sensitivity than  $^{18}\text{F}$ -DOPA PET/CT for disclosing metastases, including dissemination to the bone marrow and brain. However, CT remains the most effective imaging method for lung examination. Moreover, in the era of precision medicine, immuno-PET represents a potential theranostic molecular imaging technique to select patients for antibody-based therapy.

## DISCLOSURE

This work was supported in part by grants in 2010 from the French DHOS INCA (i.e., the French National Agency for Research) (“Investissements d’Avenir” IRON Labex no. ANR-11-LABX-0018-01 and ArronaxPlus Equipex no. ANR-11-EQPX-0004) and by a grant from SIRIC ILIAD (INCa-DGOS-Inserm\_12558). The proprietary TF2 and IMP288 reagents were provided by Immunomedics, Inc., and IBC Pharmaceuticals, Inc. David Goldenberg and Robert Sharkey own Immunomedics stock or stock options, and David Goldenberg has royalty-bearing patented inventions. David Goldenberg is the founder and retired Chairman and Chief Scientific Officer of Immunomedics, Inc., and the founder and retired Chairman of IBC Pharmaceuticals, Inc. Robert Sharkey was Senior Director of Scientific and Regulatory Affairs,

and then a consultant, to Immunomedics, Inc. No other potential conflict of interest relevant to this article was reported.

## KEY POINTS

**QUESTION:** What is the sensitivity of anti-CEA immuno-PET using the trivalent BsmAb TF2 and the  $^{68}\text{Ga}$ -IMP288 peptide in relapsing MTC patients?

**PERTINENT FINDINGS:** The overall sensitivity of immuno-PET was 92%, higher than that of  $^{18}\text{F}$ -DOPA PET/CT (65%), for disclosing metastases, including dissemination to the bone marrow and brain. CT remains the most effective imaging method for lung examination.

**IMPLICATIONS FOR PATIENT CARE:** Anti-CEA immuno-PET is an effective procedure for detecting metastatic MTC lesions and represents a potential theranostic molecular imaging technique for selecting patients to receive antibody-based therapy.

## REFERENCES

- Roy M, Chen H, Sippel RS. Current understanding and management of medullary thyroid cancer. *Oncologist*. 2013;18:1093–1100.
- Roman S, Lin R, Sosa JA. Prognosis of medullary thyroid carcinoma: demographic, clinical, and pathologic predictors of survival in 1252 cases. *Cancer*. 2006;107:2134–2142.
- Kushchayev SV, Kushchayeva YS, Tella SH, Glushko T, Pacak K, Teytelboym OM. Medullary thyroid carcinoma: an update on imaging. *J Thyroid Res*. 2019;2019:1893047.
- Wells SA, Asa SL, Dralle H, et al. Revised American Thyroid Association guidelines for the management of medullary thyroid carcinoma. *Thyroid*. 2015;25:567–610.
- Filetti S, Durante C, Hartl D, et al. Thyroid cancer: ESMO clinical practice guidelines for diagnosis, treatment and follow-up. *Ann Oncol*. 2019;30:1856–1883.
- Treglia G, Rufini V, Salvatori M, Giordano A, Giovanella L. PET imaging in recurrent medullary thyroid carcinoma. *Int J Mol Imaging*. 2012;2012:324686.
- Luster M, Karges W, Zeich K, et al. Clinical value of  $^{18}\text{F}$ -fluorine-fluorodihydroxyphenylalanine positron emission tomography/computed tomography in the follow-up of medullary thyroid carcinoma. *Thyroid*. 2010;20:527–533.
- Kauhanen S, Schalin-Jääntti C, Seppänen M, et al. Complementary roles of  $^{18}\text{F}$ -DOPA PET/CT and  $^{18}\text{F}$ -FDG PET/CT in medullary thyroid cancer. *J Nucl Med*. 2011;52:1855–1863.
- Oudoux A, Salaun P-Y, Bourmaud C, et al. Sensitivity and prognostic value of positron emission tomography with  $^{18}\text{F}$ -fluorodeoxyglucose and sensitivity of immunoscintigraphy in patients with medullary thyroid carcinoma treated with anticarcinoembryonic antigen-targeted radioimmunotherapy. *J Clin Endocrinol Metab*. 2007;92:4590–4597.
- Verbeek HHG, Plukker JTM, Koopmans KP, et al. Clinical relevance of  $^{18}\text{F}$ -FDG PET and  $^{18}\text{F}$ -DOPA PET in recurrent medullary thyroid carcinoma. *J Nucl Med*. 2012;53:1863–1871.
- Romero-Lluch AR, Cuenca-Cuenca JJ, Guerrero-Vázquez R, et al. Diagnostic utility of PET/CT with  $^{18}\text{F}$ -DOPA and  $^{18}\text{F}$ -FDG in persistent or recurrent medullary thyroid carcinoma: the importance of calcitonin and carcinoembryonic antigen cut-off. *Eur J Nucl Med Mol Imaging*. 2017;44:2004–2013.
- Giovanella L, Treglia G, Iakovou I, Mihailovic J, Verburg FA, Luster M. EANM practice guideline for PET/CT imaging in medullary thyroid carcinoma. *Eur J Nucl Med Mol Imaging*. 2020;47:61–77.
- Bailly C, Cléry P-F, Faivre-Chauvet A, et al. Immuno-PET for clinical theranostic approaches. *Int J Mol Sci*. 2016;18:57.
- Rossi EA, Goldenberg DM, Cardillo TM, McBride WJ, Sharkey RM, Chang C-H. Stably tethered multifunctional structures of defined composition made by the dock and lock method for use in cancer targeting. *Proc Natl Acad Sci USA*. 2006;103:6841–6846.
- Kraeber-Bodéré F, Rousseau C, Bodet-Milin C, et al. A pretargeting system for tumor PET imaging and radioimmunotherapy. *Front Pharmacol*. 2015;6:54.
- McBride WJ, Sharkey RM, Karacy H, et al. A novel method of  $^{18}\text{F}$  radiolabeling for PET. *J Nucl Med*. 2009;50:991–998.
- Schoffelen R, Sharkey RM, Goldenberg DM, et al. Pretargeted immuno-positron emission tomography imaging of carcinoembryonic antigen-expressing tumors with a bispecific antibody and a  $^{68}\text{Ga}$ - and  $^{18}\text{F}$ -labeled hapten peptide in mice with human tumor xenografts. *Mol Cancer Ther*. 2010;9:1019–1027.
- Bodet-Milin C, Faivre-Chauvet A, Carlier T, et al. Immuno-PET using anticarcinoembryonic antigen bispecific antibody and  $^{68}\text{Ga}$ -labeled peptide in metastatic medullary thyroid carcinoma: clinical optimization of the pretargeting parameters in a first-in-human trial. *J Nucl Med*. 2016;57:1505–1511.
- Young H, Baum R, Cremerius U, et al. Measurement of clinical and subclinical tumor response using [ $^{18}\text{F}$ ] fluorodeoxyglucose and positron emission tomography: review and 1999 EORTC recommendations. European Organization for Research and Treatment of Cancer (EORTC) PET Study Group. *Eur J Cancer*. 1999;35:1773–1782.
- Schwartz LH, Litière S, de Vries E, et al. RECIST 1.1: update and clarification—from the RECIST Committee. *Eur J Cancer*. 2016;62:132–137.
- Hadoux J, Schlumberger M. Chemotherapy and tyrosine-kinase inhibitors for medullary thyroid cancer. *Best Pract Res Clin Endocrinol Metab*. 2017;31:335–347.
- Saad MF, Fritsche HA, Samaan NA. Diagnostic and prognostic values of carcinoembryonic antigen in medullary carcinoma of the thyroid. *J Clin Endocrinol Metab*. 1984;58:889–894.
- Barbet J, Campion L, Kraeber-Bodéré F, Chatal J-F, GTE study group. Prognostic impact of serum calcitonin and carcinoembryonic antigen doubling-times in patients with medullary thyroid carcinoma. *J Clin Endocrinol Metab*. 2005;90:6077–6084.
- Lee S-W, Shim SR, Jeong SY, Kim S-J. Comparison of 5 different PET radiopharmaceuticals for the detection of recurrent medullary thyroid carcinoma: a network meta-analysis. *Clin Nucl Med*. 2020;45:341–348.
- Rousseau C, Goldenberg DM, Colombie M, et al. Initial clinical results of a novel immuno-PET theranostic probe in HER2-negative breast cancer. *J Nucl Med*. 2020;61:1205–1211.
- Treglia G, Cocciolillo F, Di Nardo F, et al. Detection rate of recurrent medullary thyroid carcinoma using fluorine-18 dihydroxyphenylalanine positron emission tomography: a meta-analysis. *Acad Radiol*. 2012;19:1290–1299.
- Castroneves LA, Coura Filho G, de Freitas RMC, et al. Comparison of  $^{68}\text{Ga}$  PET/CT to other imaging studies in medullary thyroid cancer: superiority in detecting bone metastases. *J Clin Endocrinol Metab*. 2018;103:3250–3259.
- Salaun P-Y, Campion L, Bourmaud C, et al. Phase II trial of anticarcinoembryonic antigen pretargeted radioimmunotherapy in progressive metastatic medullary thyroid carcinoma: biomarker response and survival improvement. *J Nucl Med*. 2012;53:1185–1192.
- Peltier P, Curtet C, Chatal JF, et al. Radioimmunodetection of medullary thyroid cancer using a bispecific anti-CEA/anti-indium-DTPA antibody and an indium-111-labeled DTPA dimer. *J Nucl Med*. 1993;34:1267–1273.
- Barbet J, Peltier P, Bardet S, et al. Radioimmunodetection of medullary thyroid carcinoma using indium-111 bivalent hapten and anti-CEA  $\times$  anti-DTPA-indium bispecific antibody. *J Nucl Med*. 1998;39:1172–1178.
- Chatal J-F, Campion L, Kraeber-Bodéré F, et al. Survival improvement in patients with medullary thyroid carcinoma who undergo pretargeted anti-carcinoembryonic antigen radioimmunotherapy: a collaborative study with the French Endocrine Tumor Group. *J Clin Oncol*. 2006;24:1705–1711.
- Bodet-Milin C, Ferrer L, Rauscher A, et al. Pharmacokinetics and dosimetry studies for optimization of pretargeted radioimmunotherapy in CEA-expressing advanced lung cancer patients. *Front Med (Lausanne)*. 2015;2:84.
- Schoffelen R, Woliner-van der Weg W, Visser EP, et al. Predictive patient-specific dosimetry and individualized dosing of pretargeted radioimmunotherapy in patients with advanced colorectal cancer. *Eur J Nucl Med Mol Imaging*. 2014;41:1593–1602.
- Shinmi D, Nakano R, Mitamura K, et al. Novel anticarcinoembryonic antigen antibody-drug conjugate has antitumor activity in the existence of soluble antigen. *Cancer Med*. 2017;6:798–808.
- Dotan E, Cohen SJ, Starodub AN, et al. Phase I/II trial of labezumab govitecan (anti-CEACAM5/SN-38 antibody-drug conjugate) in patients with refractory or relapsing metastatic colorectal cancer. *J Clin Oncol*. 2017;35:3338–3346.